

Green's function of a dressed particle

Mona Berciu

Department of Physics and Astronomy, University of British Columbia, Vancouver, BC V6T 1Z1, Canada
(Dated: March 23, 2022)

We present a new, highly efficient yet accurate approximation for the Green's functions of dressed particles, using the Holstein polaron as an example. Instead of summing a subclass of diagrams (*e.g.* the non-crossed ones, in the self-consistent Born approximation (SCBA)), we *sum all the diagrams*, but with each diagram averaged over its free propagators' momenta. The resulting Green's function satisfies exactly the first six spectral weight sum rules. All higher sum rules are satisfied with great accuracy, becoming asymptotically exact for coupling both much larger and much smaller than the free particle bandwidth. Possible generalizations to other models are also discussed.

PACS numbers: 71.38.-k, 72.10.Di, 63.20.Kr

One of the most fundamental problems in both high-energy and condensed matter physics is to understand what happens when a particle couples to an environment, in particular what are the properties of the resulting object, consisting of the bare particle dressed by a cloud of excitations. This type of problem arises again and again as couplings to new kinds of environments are studied.

The most desirable quantity to know is the Green's function $G(\vec{k}, \omega)$ of the dressed particle – its poles mark the eigenspectrum, while the associated residues contain information on the eigenfunctions. Moreover, the spectral weight $A(\vec{k}, \omega) = -\frac{1}{\pi} \text{Im} G(\vec{k}, \omega)$ can be directly measured experimentally using Angle-Resolved Photoemission Spectroscopy [1]. Recently, such work has reignited a debate on whether the carriers in high- T_c cuprates are polarons, that is, electrons dressed by phonons [2].

$G(\vec{k}, \omega)$ is the sum of an infinite number of diagrams corresponding to an expansion to all orders in the coupling strength [3]. Diagrammatic Monte Carlo (DMC) can perform the *numerical* summation of all diagrams [4]. Other ways to find $G(\vec{k}, \omega)$ are from exact diagonalizations (ED) of small systems, variational methods, Density Matrix Renormalization Group in one-dimension, etc [5, 6, 7, 8]. However, these methods require considerable computational resources, are time consuming, and often limit themselves to finding only the low-energy properties, such as the ground-state energy.

To our knowledge, there are only two easy-to-estimate approximations for $G(\vec{k}, \omega)$. One is the SCBA which consists in summing only the non-crossed diagrams. Because the percentage of diagrams kept decreases fast with increasing order, SCBA fails badly at strong couplings. The other approximation, obtained from a modified Lang-Firsov (MLF) approach [9], is exact both for

zero coupling and for zero bandwidth, however results for finite bandwidth/coupling are rather poor (see below).

In this Letter we find a new approximation for $G(\vec{k}, \omega)$, which is as easy to estimate as SCBA and MLF, but is *highly accurate over most of the parameter space*. We validate this both by comparison against numerical results, and by investigating its sum rules. Most of the discussion here is limited to the Holstein model, for which many numerical results are available. Possible generalizations for other models are briefly discussed at the end.

Consider the Holstein Hamiltonian:

$$\mathcal{H} = \sum_{\vec{k}} (\epsilon_{\vec{k}} c_{\vec{k}}^\dagger c_{\vec{k}} + \omega_E b_{\vec{k}}^\dagger b_{\vec{k}}) + \frac{g}{\sqrt{N}} \sum_{\vec{k}, \vec{q}} c_{\vec{k}-\vec{q}}^\dagger c_{\vec{k}} (b_{\vec{q}}^\dagger + b_{-\vec{q}}) \quad (1)$$

which contains the kinetic energy of the free particle (electron), a branch of Einstein bosons (optical phonons) and the linear coupling between particle and bosons. When needed, we use $\epsilon_{\vec{k}} = -2t \sum_{\alpha=1}^d \cos(k_\alpha a)$, for nearest-neighbor hopping on a d -dimensional cubic lattice with N sites and lattice constant a . The spin of the particle and whether it is a boson or a fermion is irrelevant. Sums over momenta are over the first Brillouin zone (BZ), $-\frac{\pi}{a} < k_\alpha \leq \frac{\pi}{a}$, $\alpha = 1, d$.

The one-particle Green's function of a M -particle system is $G(\vec{k}, \tau) = -i \langle \Phi_M | T[c_{\vec{k}}(\tau) c_{\vec{k}}^\dagger(0)] | \Phi_M \rangle$, with $|\Phi_M\rangle$ the M -particle ground-state, T the time ordering operator, and $c_{\vec{k}}(\tau) = \exp(i\mathcal{H}\tau) c_{\vec{k}} \exp(-i\mathcal{H}\tau)$ (we set $\hbar = 1$) [3]. The spectrum of a single dressed particle (polaron) is obtained for $M = 0$. The ground state (GS) in the absence of particles is the vacuum $|\Phi_0\rangle = |0\rangle$, and since $\mathcal{H}|0\rangle = 0$, the polaron's Green's function simplifies to:

$$G(\vec{k}, \tau) = -i\Theta(\tau) \langle 0 | c_{\vec{k}} e^{-i\mathcal{H}\tau} c_{\vec{k}}^\dagger | 0 \rangle \quad (2)$$

where $\Theta(\tau)$ is the Heaviside function. From Eqs. (1) and (2), we derive the equation of motion:

$$i \frac{d}{d\tau} G(\vec{k}, \tau) = \delta(\tau) + \epsilon_{\vec{k}} G(\vec{k}, \tau) + \frac{g}{\sqrt{N}} \sum_{\vec{q}_1} F_1(\vec{k}, \vec{q}_1, \tau)$$

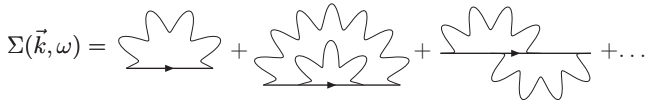


FIG. 1: Diagrammatics for Σ , where $G = G_0 + G_0 \Sigma G$.

where $F_1(\vec{k}, \vec{q}_1, \tau) = -i\Theta(\tau)\langle 0|c_{\vec{k}}^\dagger \exp(-i\mathcal{H}\tau)c_{\vec{k}-\vec{q}_1}^\dagger b_{\vec{q}_1}^\dagger|0\rangle$. Continuing in this vein, we generate an infinite hierarchy of coupled equations of motion for the Green's functions $F_n(\vec{k}, \vec{q}_1, \dots, \vec{q}_n, \tau) = -i\Theta(\tau)\langle 0|c_{\vec{k}}^\dagger e^{-i\mathcal{H}\tau}c_{\vec{k}-\vec{q}_T}^\dagger b_{\vec{q}_1}^\dagger \dots b_{\vec{q}_n}^\dagger|0\rangle$, with $\vec{q}_T = \sum_{i=1}^n \vec{q}_i$ and $G(\vec{k}, \tau) = F_0(\vec{k}, \tau)$. In the frequency domain, these equations of motion become:

$$G(\vec{k}, \omega) = G_0(\vec{k}, \omega)[1 + \frac{g}{\sqrt{N}} \sum_{\vec{q}_1} F_1(\vec{k}, \vec{q}_1, \omega)] \quad (3)$$

and for any $n \geq 1$,

$$\begin{aligned} F_n(\vec{k}, \vec{q}_1, \dots, \vec{q}_n, \omega) &= \frac{g}{\sqrt{N}} G_0(\vec{k} - \vec{q}_T, \omega - n\omega_E) \\ &\times [\sum_{i=1}^n F_{n-1}(\vec{k}, \vec{q}_1, \dots, \vec{q}_{i-1}, \vec{q}_{i+1}, \dots, \vec{q}_n, \omega) \\ &+ \sum_{\vec{q}_{n+1}} F_{n+1}(\vec{k}, \vec{q}_1, \dots, \vec{q}_n, \vec{q}_{n+1}, \omega)] \quad (4) \end{aligned}$$

where $G_0(\vec{k}, \omega) = [\omega - \epsilon_{\vec{k}} + i\eta]^{-1}$ is the non-interacting one-particle Green's function. This system generates the expected diagrammatic expansion for the self-energy $\Sigma(\vec{k}, \omega) = G_0^{-1}(\vec{k}, \omega) - G^{-1}(\vec{k}, \omega)$, shown in Fig. 1.

Let $f_n(\vec{k}, \omega) = N^{-n} \sum_{\vec{q}_1, \dots, \vec{q}_n} F_n(\vec{k}, \vec{q}_1, \dots, \vec{q}_n, \omega)$. In terms of these, Eq. (3) becomes $G(\vec{k}, \omega) = G_0(\vec{k}, \omega)[1 + g\sqrt{N}f_1(\vec{k}, \omega)]$. The equations for $f_n(\vec{k}, \omega)$, $n \geq 1$, are obtained by summing Eqs. (4) over all phonon momenta. Of the two terms on the right-hand side, the first one can be expressed in terms of $f_{n-1}(\vec{k}, \omega)$ exactly, but the second one requires an approximation. We replace:

$$\begin{aligned} \sum_{\vec{q}_1, \dots, \vec{q}_{n+1}} G_0(\vec{k} - \vec{q}_T, \omega - n\omega_E) F_{n+1}(\vec{k}, \vec{q}_1, \dots, \vec{q}_{n+1}, \omega) \\ \approx N^{n+1} \bar{g}_0(\omega - n\omega_E) f_{n+1}(\vec{k}, \omega) \quad (5) \end{aligned}$$

where

$$\bar{g}_0(\omega) = \frac{1}{N} \sum_{\vec{k}} G_0(\vec{k}, \omega) \quad (6)$$

The justification is that $\vec{q}_T = \sum_{i=1}^n \vec{q}_i$ takes, with equal probability, any value in the first Brillouin zone. Replacing $G_0(\vec{k} - \vec{q}_T, \omega - n\omega_E) \rightarrow \langle G_0(\vec{k} - \vec{q}_T, \omega - n\omega_E) \rangle_{\vec{q}_T} = \bar{g}_0(\omega - n\omega_E)$ allows us to also write this term as a function of $f_{n+1}(\vec{k}, \omega)$ only. We discuss below the meaning of this momentum average (MA) in terms of diagrams; however, note that for hopping $t = 0$ this MA approximation becomes exact, because for $t = 0$ all Green's functions are independent of momenta. This suggests that MA should be valid at least in the strong-coupling regime $t/g \ll 1$. As we show later, its validity range is in fact much wider.

With this approximation, Eqs. (4) become $f_n(\vec{k}, \omega) = \bar{g}_0(\omega - n\omega_E) \left[\frac{ng}{\sqrt{N}} f_{n-1}(\vec{k}, \omega) + g\sqrt{N} f_{n+1}(\vec{k}, \omega) \right]$. This recursive chain has a continued-fraction solution. The resulting Green's function can be cast in the usual form

$G_{MA}(\vec{k}, \omega) = [\omega - \epsilon_{\vec{k}} - \Sigma_{MA}(\omega) + i\eta]^{-1}$, where:

$$\Sigma_{MA}(\omega) = \frac{g^2 \bar{g}_0(\omega - \omega_E)}{1 - \frac{2g^2 \bar{g}_0(\omega - \omega_E) \bar{g}_0(\omega - 2\omega_E)}{1 - \frac{3g^2 \bar{g}_0(\omega - 2\omega_E) \bar{g}_0(\omega - 3\omega_E)}{1 - \dots}}} \quad (7)$$

As pointed already out, if $t = 0$, in which case $\bar{g}_0(\omega) = (\omega + i\eta)^{-1}$, this expression is exact. Indeed, one can show [10] that it equals the expected Lang-Firsov result [3] [$\lambda = (g/\omega_E)^2$]:

$$G(\omega) = e^{-\lambda} \sum_{n=0}^{\infty} \frac{\lambda^n}{n!} \frac{1}{\omega + \lambda\omega_E - n\omega_E + i\eta} \quad (8)$$

This mapping was used before in a Dynamical Mean Field Theory (DMFT) study of this problem, which also produces an approximation for the Green's function [7]. In fact, Eq. (7) looks similar to $\Sigma_{DMFT}(\omega)$; however, our $\bar{g}_0(\omega)$ is *not* a solution of the self-consistent DMFT equations (except at $t = 0$ and $g = 0$, where both methods are exact). At finite g/t the two self-energies are different. Moreover, because of the limit $d \rightarrow \infty$, in DMFT G itself (not only Σ) is independent of \vec{k} . Finally, the DMFT evaluation requires self-consistent iterations, and is therefore much more involved than that of the MA, SCBA and MLF. For these reasons, we do not consider the results of the DMFT in the following.

Interestingly, SCBA also depends on $\bar{g}_0(\omega)$. Since $\Sigma_{SCBA}(\omega) = \frac{g^2}{N} \sum_q G_{SCBA}(k - q, \omega - \omega_E)$, we have:

$$\begin{aligned} \Sigma_{SCBA}(\omega) &= g^2 \bar{g}_0(\omega - \omega_E - \Sigma_{SCBA}(\omega - \omega_E)) \\ &= g^2 \bar{g}_0(\omega - \omega_E - g^2 \bar{g}_0(\omega - 2\omega_E - g^2 \bar{g}_0(\omega - 3\omega_E - \dots))) \end{aligned}$$

On the other hand, for the Holstein model, the MLF expression is reminiscent of Eq. (8) [9, 11]:

$$G_{MLF}(\vec{k}, \omega) = e^{-\lambda} \sum_{n=0}^{\infty} \frac{\lambda^n}{n!} \frac{1}{\omega - e^{-\lambda} \epsilon_{\vec{k}} + \lambda\omega_E - n\omega_E + i\eta}$$

To understand the diagrammatic meaning of the MA approximation, we expand Eq. (7) in powers of g^2 :

$$\begin{aligned} \Sigma_{MA}(\omega) &= g^2 \bar{g}_0(\omega - \omega_E) + g^4 2\bar{g}_0^2(\omega - \omega_E) \bar{g}_0(\omega - 2\omega_E) \\ &+ g^6 [4\bar{g}_0^3(\omega - \omega_E) \bar{g}_0^2(\omega - 2\omega_E) + 6\bar{g}_0^2(\omega - \omega_E) \\ &\times \bar{g}_0^2(\omega - 2\omega_E) \bar{g}_0(\omega - 3\omega_E)] + \mathcal{O}(g^8) \quad (9) \end{aligned}$$

showing one contribution of order g^2 (which is the correct Born expression), 2 of order g^4 , 10 of order g^6 , etc. One can verify that this generates the correct total number of diagrams in all orders. The difference is that in all MA diagrams, each $G_0(\vec{p}, \Omega)$ free propagator is replaced by a momentum averaged $\bar{g}_0(\Omega)$ function. For example, the exact 2^{nd} order contribution (see Fig. 1):

$$\begin{aligned} \frac{g^4}{N^2} \sum_{\vec{q}_1, \vec{q}_2} G_0(\vec{k} - \vec{q}_1, \omega - \omega_E) G_0(\vec{k} - \vec{q}_1 - \vec{q}_2, \omega - 2\omega_E) \\ \times [G_0(\vec{k} - \vec{q}_1, \omega - \omega_E) + G_0(\vec{k} - \vec{q}_2, \omega - \omega_E)] \quad (10) \end{aligned}$$

is replaced within the MA approximation by

$$2g^4 \left(\frac{1}{N} \sum_{\vec{q}_1} G_0(\vec{q}_1, \omega - \omega_E) \right)^2 \left(\frac{1}{N} \sum_{\vec{q}_2} G_0(\vec{q}_2, \omega - 2\omega_E) \right) \quad (11)$$

All higher orders are obtained similarly. Let us see why this is indeed a good approximation if $t \ll g$. If $t = 0$, the two expressions are equal. Higher order powers of t come from expanding each $G_0(\vec{k}, \omega) = G_0(\omega) + \epsilon_{\vec{k}} G_0^2(\omega) + \dots$, where $G_0(\omega) = (\omega + i\eta)^{-1}$. All odd-order powers are zero since $\sum_{\vec{k}} \epsilon_{\vec{k}}^{2n+1} = 0$. Consider $\mathcal{O}(t^2)$ terms in Eq. (10): these come either from expanding one of the G_0 to $\mathcal{O}(t^2)$, in which case they equal their counterparts in Eq. (11); or they come from $\mathcal{O}(t)$ contributions from two different G_0 lines. In the later case, most terms are zero because the two lines generally carry different momenta, and $\sum_{\vec{q}_1, \vec{q}_2} \epsilon_{\vec{q}_1} \epsilon_{\vec{q}_2} = 0$. Of 6 such terms generated in Eq. (10), only one, coming from the outside G_0 lines of the non-crossed diagram, is finite. The error from such terms decreases as one goes to higher order diagrams, because the percentage of diagrams with one or more pairs of G_0 lines of equal momenta decreases exponentially. Similar arguments apply for higher powers in t . It follows that MA captures most of the t dependence of each diagram, while summing over all diagrams. This suggests that MA may be accurate even far from the limit $t \ll g$. Indeed, Eq. (9) clearly shows that MA is also valid for $g \ll t$.

For a better idea of the accuracy and range of the MA, we consider the sum rules for $A(\vec{k}, \omega) \equiv -\frac{1}{\pi} \text{Im} G(\vec{k}, \omega)$, $M_n(\vec{k}) \equiv \int_{-\infty}^{\infty} d\omega \omega^n A(\vec{k}, \omega)$, which can be evaluated analytically. The usual approach [11] is based on the equations of motion; since MA is also based on them, it should fare well. Another approach [10] is to start with the Dyson equation $G(\vec{k}, \omega) = G_0(\vec{k}, \omega) + G_0^2(\vec{k}, \omega) \Sigma(\vec{k}, \omega) + G_0^3(\vec{k}, \omega) \Sigma^2(\vec{k}, \omega) + \dots$ and the perturbational expansion $\Sigma(\vec{k}, \omega) = g^2 \Sigma^{(1)}(\vec{k}, \omega) + g^4 \Sigma^{(2)}(\vec{k}, \omega) + \dots$, perform the integrals $\int_{-\infty}^{\infty} d\omega \omega^n G(\vec{k}, \omega)$ and then take the imaginary part. This task is aided by the fact that most terms in the integrand decay faster than $1/\omega$ as $\omega \rightarrow \infty$, and their contributions vanish. For $n = 0, 1$, only $G_0(\vec{k}, \omega)$ has finite contributions, giving $M_0(\vec{k}) = 1$; $M_1(\vec{k}) = \epsilon_{\vec{k}}$. In fact, G_0 contributes an $\epsilon_{\vec{k}}^n$ to $M_n(\vec{k})$. Next is $G_0^2 g^2 \Sigma^{(1)}$. It decays like $1/\omega^3$, so it contributes only for $n \geq 2$. Both SCBA and MA have the exact expression for $\Sigma^{(1)}$, so they both satisfy exactly the $n = 2$ and 3 sum rules. For $n \geq 4$, both $G_0^2 g^4 \Sigma^{(2)}$ and $G_0^3 (g^2 \Sigma^{(1)})^2$ contribute. Since SCBA ignores one $\Sigma^{(2)}$ diagram, it fails at this point, while MA is still exact for $n = 4$ and 5. MA fails at $n = 6$ because of the approximations in diagrams' expressions. Instead of $M_6(\vec{k}) = \epsilon_{\vec{k}}^6 + g^2 [5\epsilon_{\vec{k}}^4 + 6t^4(2d^2 - d) + 4\epsilon_{\vec{k}}^3 \omega_E + 3\epsilon_{\vec{k}}^2 \omega_E^2 + 6dt^2(\epsilon_{\vec{k}}^2 + 2\epsilon_{\vec{k}} \omega_E + 2\omega_E^2) + 2\epsilon_{\vec{k}} \omega_E^3 + \omega_E^4] + g^4(18dt^2 + 12\epsilon_{\vec{k}}^2 + 22\epsilon_{\vec{k}} \omega_E + 25\omega_E^2) + 15g^6$, MA predicts a sum rule equal to $M_6(\vec{k}) - 2dt^2 g^4$ (the dimension d enters through $2dt^2 = \frac{1}{N} \sum_{\vec{k}} \epsilon_{\vec{k}}^2$ and higher averages). In other

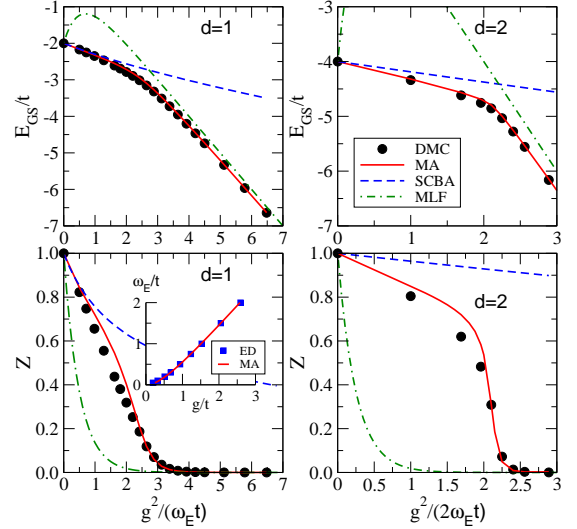


FIG. 2: GS energy, E_{GS} , and quasiparticle weight, Z , for $\omega_E = 0.5t$. $d = 1$ (left) and $d = 2$ (right). Inset: line below which a second bound peak appears in 1d (see text).

words, MA captures *exactly* both the dominant power in t , $\epsilon_{\vec{k}}^n$, and the dominant power in g , which is $\sim g^n$ or $\omega_E g^{n-1}$, for even/odd n . This also follows because MA is exact both for $t = 0$ and $g = 0$, so it can only miss terms $\sim g^4 t^2$. These are lost because terms from G_0 lines carrying equal momenta are neglected. As discussed, such terms are a small minority of all contributions, and indeed MA recovers the vast majority of terms in any M_n , like in the $n = 6$ case, showing that it is highly accurate not only for $t \ll g$ and $t \gg g$, but also for intermediary values. By contrast, although exact up to $n = 3$, SCBA fails badly at higher n because of the many higher order diagrams it neglects. For example, for $n = 6$, SCBA predicts $5g^6$ instead of $15g^6$ as the leading g term (with many $\mathcal{O}(g^4)$ terms missing), showing that SCBA fails for $g \gg t$. Following this analysis we conclude that agreement with a few sum rules is not meaningful; meaningful is to have agreement for the vast majority of terms in *all* sum rules, and in particular for the dominant terms in various limits. MA satisfies this restrictive condition.

MLF also captures both the $t = 0$ and the $g = 0$ limits exactly. However, this alone does not suffice, either. Direct evaluation shows that MLF fails badly all sum rules with $n \geq 1$ if $g \neq 0$, as it predicts $M_1 \rightarrow e^{-\lambda} \epsilon_{\vec{k}}$, etc.

A comparison of MA, SCBA and MLF against GS energies and qp weights $Z = |\langle GS | c_{\vec{k}=0}^\dagger | 0 \rangle|^2$ obtained with DMC [12] are shown in Fig. 2, for both $d = 1$ and 2. MA compares equally well throughout the Brillouin zone [10]. The agreement is best for $g \ll t$ and $g \gg t$, but is good even for $g \sim t$. In the inset, we show the line in parameter space below which a second bound peak appears in 1d (*i.e.* the energy of the first excited $k = 0$ state satisfies $E_1 < E_{GS} + \omega_E$). Above this line, a continuum starts at $E_{GS} + \omega_E$. The agreement between MA and ED data of

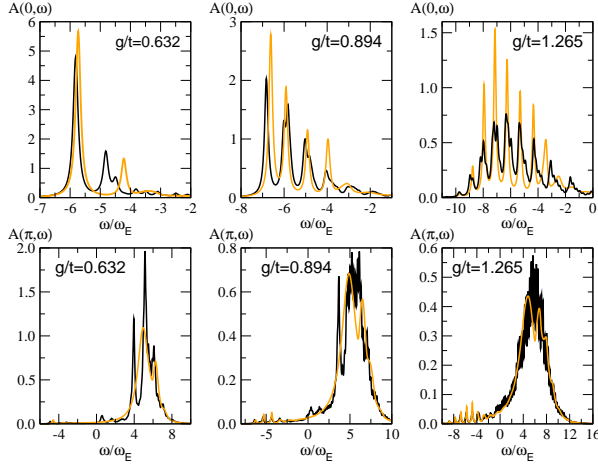


FIG. 3: (Color online) $A(k, \omega)$ in 1d, for $t = 1, \omega_E = 0.4, \eta = 0.1\omega_E, g = 0.632, 0.894$ and 1.265 , and $k = 0$ and π . MA data (orange line) vs. results from Ref. [8] (black line).

Ref. [6] is excellent. By contrast, SCBA never predicts a second bound state (it always finds the continuum); MLF always predicts a peak at $E_{GS} + \omega_E$, never a continuum.

A comparison of the MA spectral weight $A(k, \omega)$ (orange line) in 1d, for $k = 0$ and π/a and three values of g is shown in Fig. 3, against data (black line) based on a variational method [8]. The agreement is again decent, especially since $g \sim t$ in all three cases. Other comparisons with numerical data are of similar quality [10].

MA thus provides an accurate, yet simple and fast way to study $G(\vec{k}, \omega)$ for Holstein polarons in any dimension for any $\epsilon_{\vec{k}}$. The question is whether this approach can be expanded beyond the Holstein Hamiltonian. While this issue is still under investigation [10], one possible route is provided by this generalization of Eq. (7):

$$\tilde{\Sigma}(\vec{k}, \omega) = \frac{1}{N} \sum_{\vec{q}_1, \lambda_1} \frac{E_1(\vec{k}, \vec{q}_1, \lambda_1)}{1 - \frac{1}{N} \sum_{\vec{q}_2, \lambda_2} \frac{E_2(\vec{k}, \vec{q}_1, \vec{q}_2, \lambda_1, \lambda_2)}{1 - \dots}} \quad (12)$$

$E_1(\vec{k}, \vec{q}_1, \lambda_1) = |g_{\vec{k}, \vec{q}_1, \lambda_1}|^2 G_0(\vec{k}_1, \omega_1)$, $E_2(\vec{k}, \vec{q}_1, \vec{q}_2, \lambda_1, \lambda_2) = |g_{\vec{k}_1, \vec{q}_2, \lambda_2}|^2 G_0(\vec{k}_{1,2}, \omega_{1,2}) (G_0(\vec{k}_1, \omega_1) + G_0(\vec{k}_2, \omega_2))$, etc, where $\vec{k}_i = \vec{k} - \vec{q}_i$, $\vec{k}_{1,2} = \vec{k} - \vec{q}_1 - \vec{q}_2$ and $\omega_i = \omega - \omega_{\vec{q}_i, \lambda_i}$, $\omega_{1,2} = \omega - \omega_{\vec{q}_1, \lambda_1} - \omega_{\vec{q}_2, \lambda_2}$. This describes coupling to several branches of bosons with dispersions $\omega_{\vec{q}\lambda}$, with a vertex $g_{\vec{k}, \vec{q}\lambda}$ if \vec{k} is the momentum of the incoming particle and $\vec{q}\lambda$ is the momentum and branch of the emitted boson. While not exact, $\tilde{\Sigma}(\vec{k}, \omega)$ is much more accurate than Σ_{MA} : it gives all 1st, 2nd and 9 out of 10 of the 3rd order diagrams exactly. The wrong 3rd order diagram has one of its five G_0 lines with a wrong momentum and energy. All higher order diagrams' numbers and topologies are generated correctly, a small fraction of them having some mislabelled G_0 lines. One can trace the first failing of a sum rule, due to the wrong 3rd order diagram, to now

occur in $M_8(\vec{k})$. For simplicity, let us assume that boson frequencies ω_λ and vertices g_λ depend only on the branch. Then, in $M_8(\vec{k})$, a term $\langle |g_\lambda|^2 \rangle \langle \omega_\lambda | g_\lambda |^2 \rangle^2$ is replaced by $\langle |g_\lambda|^2 \rangle^2 \langle \omega_\lambda^2 | g_\lambda |^2 \rangle$, and an extra term $2dt^2 \langle |g_\lambda|^2 \rangle^3$ is generated, but all other terms including the dominant g terms $105 \langle |g_\lambda|^2 \rangle^4$ are exact (here, $\langle f \rangle = \sum_\lambda f$). Using a further MA approximation removes the need to evaluate the momentum sums in (12) by replacing all $G_0(\vec{p}, \Omega) \rightarrow \bar{g}_0(\Omega)$; this results in an error in $M_6(\vec{k})$ (a missing $2dt^2 \langle |g_\lambda|^2 \rangle^2$) but would speed up calculations significantly and, as for the Holstein model, should have a limited effect on accuracy. Further simplifications are possible if the boson frequencies are close to each other. One can show that if $t = 0$ and all $\omega_\lambda = \omega_E$, Eq. (7) with $g^2 = \langle |g_\lambda|^2 \rangle$ is the *exact* self-energy [10]. We do not know if this identity has been noted before. For close-by phonon energies, one can then also remove the branch sums in (12) by using Eq. (7) with $g^2 = \langle |g_\lambda|^2 \rangle$, $\omega_E = \langle \omega_\lambda | g_\lambda |^2 \rangle / g^2$, in which case one gets an error starting with $M_4(\vec{k})$, where $\langle \omega_\lambda^2 | g_\lambda |^2 \rangle \rightarrow g^2 \omega_E^2$, but all dominant terms are correct in all orders. Eq. (12) may also be easy to estimate for highly anisotropic $g_{\vec{q}}$, in which case the BZ sums reduce to summations over a few hot spots. Of course, tests against numerical results are needed to verify all this.

To conclude, progress has been made in a very old problem, by finding a simple yet highly accurate approximation for $G(\vec{k}, \omega)$ of the Holstein polaron. A path to possibly more exciting results has also been uncovered.

Acknowledgments: I thank George Sawatzky for suggesting this problem and for many useful discussions, and A. Macridin, V. Cataudella and G. De Filippis for sharing their numerical results. This work was supported by NSERC and CIAR Nanoelectronics of Canada.

-
- [1] A. Damascelli, Z. Hussain, and Z.-X. Shen, Rev. Mod. Phys. **75**, 473 (2003).
 - [2] K. M. Shen *et al.*, Phys. Rev. Lett. **93**, 267002 (2004).
 - [3] G. D. Mahan, *Many-Particle Physics*, (Plenum, New York, 1981).
 - [4] N. V. Prokof'ev and B. V. Svistunov, Phys. Rev. Lett. **81**, 2514 (1998).
 - [5] E. Jeckelmann and S. R. White, Phys. Rev. B **57**, 6376 (1998); A. H. Romero, D. W. Brown, and K. Lindenberg, Phys. Rev. B **59**, 13728 (1999); V. Cataudella, G. De Filippis, and G. Iadonisi, Phys. Rev. B **62**, 1496 (2000).
 - [6] J. Bonca, S. A. Trugman, and I. Batistic, Phys. Rev. B **60**, 1633 (1999).
 - [7] S. Ciuchi *et al.*, Phys. Rev. B **56**, 4494 (1997).
 - [8] G. De Filippis *et al.*, Phys. Rev. B **72**, 014307 (2005).
 - [9] A. S. Alexandrov and J. Ranninger, Phys. Rev. B **45**, 13109 (1992).
 - [10] M. Berciu, unpublished.
 - [11] P. E. Kornilovitch, EuroPhys Lett. **59**, 735 (2002).
 - [12] A. Macridin, Ph.D. Thesis, Rijkuniversiteit Gröningen, 2003.